Scope and limitations of flash pyrolysis–gas chromatography/mass spectrometry as revealed by the thermal behaviour of high-molecular-weight lipids derived from the green microalga *Botryococcus braunii* [1]

François Gelin [a,*], Jan W. de Leeuw [b], Jaap S. Sinninghe Damsté [b], Sylvie Derenne [c], Claude Largeau [c] and Pierre Metzger [c]

[a] *Delft University of Technology, Faculty of Chemical Technology and Materials Science, Organic Geochemistry Unit, de Vries van Heysplantsoen 2, 2628 RZ Delft (The Netherlands)*
[b] *Netherlands Institute of Sea Research (NIOZ), Division of Marine Biogeochemistry, P.O. Box 59, 1790 AB den Burg, Texel (The Netherlands)*
[c] *Laboratoire de Chimie Bioorganique et Organique Physique, UA CNRS 1381, ENSCP, 11 rue Pierre et Marie Curie, 75231 Paris Cedex 05 (France)*

ABSTRACT

Curie point pyrolysis–gas chromatography/mass spectrometry studies of four types of high-molecular-weight (HMW) lipids isolated from the green microalga *Botryococcus braunii* race A were performed to determine the thermal behaviour of these lipids and to propose mechanisms of pyrolysis for these types of compounds. Although two types of lipids induced detectable pyrolysis products upon heating of the ferromagnetic wires at Curie temperatures of 610 and 770°C, transfer problems from the pyrolysis unit to the GC column were observed. Therefore, further analysis of the pyrolysis residues is suggested. Furthermore, two types of lipids presenting long alkyl chains (up to C_{64}) did not pyrolyse under the experimental conditions but were thermally extracted from the wire at any of the tested temperatures. Some of these HMW lipids could, however, be analysed by high-temperature gas chromatography (temperatures up to 375°C). Mechanisms of pyrolysis, partly based on previous studies, were proposed for the two types of ether lipids. These mechanisms allowed the structural reconstruction of the main biopolymer that composes the cell outer walls of the microalga *B. braunii* race L. This biomacromolecule was found to be comprised of C_{40} isoprenoid (lycopene) units, ether linked at the C(14) and C(15) positions.

Botryococcus braunii; flash pyrolysis; high-molecular-weight lipids; high-temperature gas chromatography; PRB L; pyrolysis.

INTRODUCTION

Flash pyrolysis–gas chromatography (Py–GC) and flash pyrolysis-gas chromatography/mass spectrometry (Py–GC/MS) have been used successfully in organic geochemistry and petroleum geochemistry to structurally characterise macromolecular organic substances in source rocks, kerogens, crude oils, coals and soils [1,2]. Recently, Py–GC/MS analyses of these materials have resulted in a major reappraisal of the formation of "geopolymers" and have contributed to our understanding of crude oil formation [3,4]. It has become clear that resistant highly aliphatic biomacromolecules derived from algal cell walls, plant cuticles, seeds and periderm plant tissues are sometimes significant constituents of "geopolymers". Reversibly, pyrolysis data of kerogens have contributed significantly to the recognition of these resistant aliphatic macromolecules in organisms [5,6].

To further increase our understanding of kerogen, coal and crude oil formation, it is a prerequisite to understand better mechanisms of pyrolysis of these aliphatic macromolecules. Since the highly aliphatic biopolymers in cell walls of several races of the microalga *Botryococcus braunii* contribute significantly to many kerogens in source rocks (sometimes the kerogens consist mainly of these materials, e.g. Torbanites [7,8], Coorongites [9,10] and Ribesalbes oil shale [11]), detailed pyrolysis studies of isolated and purified biopolymers and related high-molecular-weight (HMW) lipids of *B. braunii* have been performed recently [10,12,13]. These studies also helped to clarify mechanisms of pyrolysis since the structures of HMW lipids isolated from these algae are well characterised [14].

During the initial stages of the work described here, erroneous results were observed upon Py–GC/MS studies of a new series of complex lipids isolated from *B. braunii* race A. Therefore a more detailed study was undertaken to understand better the pitfalls and limitations of Py–GC/MS analyses of these materials.

Furthermore, thanks to this and earlier studies concerning mechanisms of pyrolysis of ether lipids isolated from *B. braunii*, it was possible to reconstruct the detailed macromolecular structure of the insoluble aliphatic cell wall biopolymer of *B. braunii* race L.

EXPERIMENTAL

Origin and isolation of high-molecular-weight lipids

The four series of compounds investigated were recovered from different strains of *B. braunii* race A by hexane extraction. Silica gel column chromatography, TLC and HPLC of this hexane extract allowed for the isolation of series of related and individual compounds [15–17].
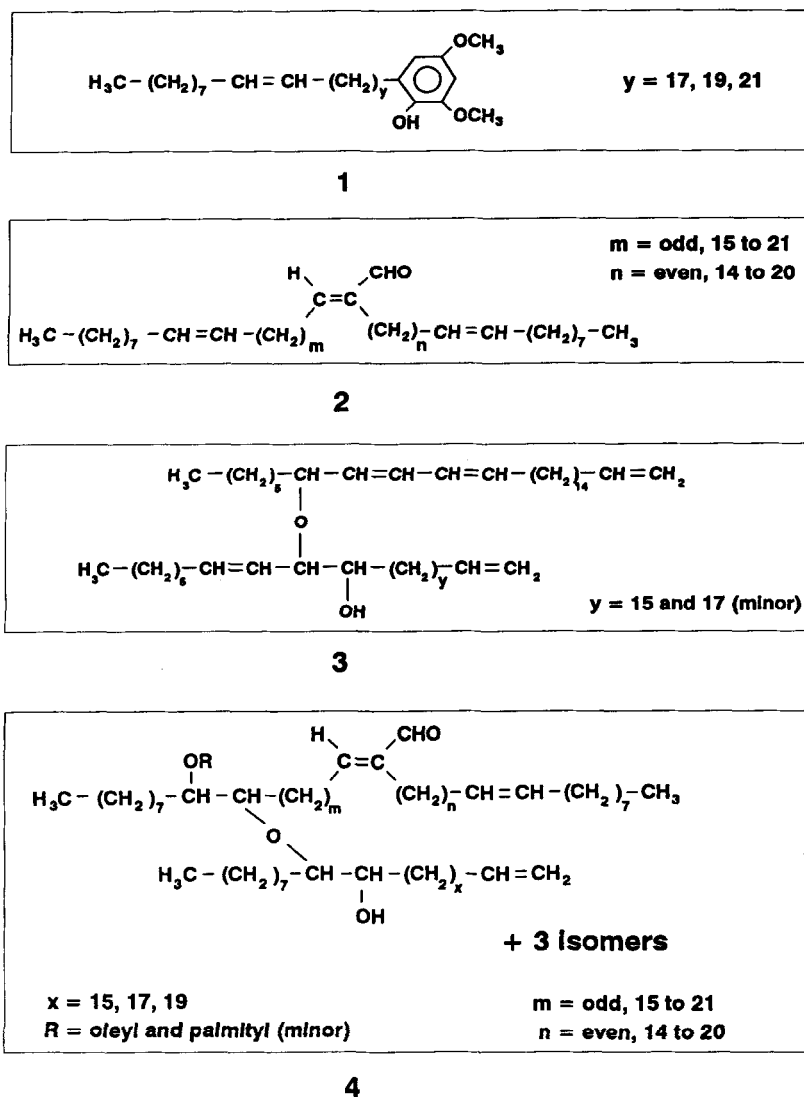
$$H_3C-(CH_2)_7-CH=CH-(CH_2)_y-\text{[ring: OCH}_3\text{, OH, OCH}_3\text{]}$$

y = 17, 19, 21

1

m = odd, 15 to 21
n = even, 14 to 20

$$H_3C-(CH_2)_7-CH=CH-(CH_2)_m-C=C(H)(CHO)-(CH_2)_n-CH=CH-(CH_2)_7-CH_3$$

2

$$H_3C-(CH_2)_5-CH-CH=CH-CH=CH-(CH_2)_{14}-CH=CH_2$$
$$|$$
$$O$$
$$|$$
$$H_3C-(CH_2)_5-CH=CH-CH-CH-(CH_2)_y-CH=CH_2$$
$$|$$
$$OH$$

y = 15 and 17 (minor)

3

$$H_3C-(CH_2)_7-CH(OR)-CH-(CH_2)_m-C=C(H)(CHO)-(CH_2)_n-CH=CH-(CH_2)_7-CH_3$$
$$\backslash O \backslash$$
$$H_3C-(CH_2)_7-CH-CH-(CH_2)_x-CH=CH_2$$
$$|$$
$$OH$$

+ 3 isomers

x = 15, 17, 19
R = oleyl and palmityl (minor)

m = odd, 15 to 21
n = even, 14 to 20

4

Fig. 1. Structures of the four series of lipids studied [14].

6-n-Alkenyl-2,4-dimethoxyphenols (1; Fig. 1) and botryals (2; Fig. 1) have both been detected in almost all strains of *B. braunii* race A investigated so far. Compounds 1 were isolated from a collection strain from Austin (TX) and accounted for approx. 1.5% of dry algal biomass [15]. Compounds 2 were isolated from the Austin strain and accounted for 9.9% of dry biomass [15].

The alkatrienyl–alkadienyl ether (3; Fig. 1) was found in two strains of the race A originating from the Bolivian Lake Overjuyo and the French Lake Coat ar Herno [16]. Compounds 3 accounted for up to 26% of the dry

biomass in laboratory cultures. The botryal–alkenyl ethers (4; Fig. 1) were isolated from the Austin strain and accounted for 1% of the dry biomass [17].

A review by Metzger et al. [14] describes in detail the different methods used for the structural identification of the lipids shown in Fig. 1.

Isolation of the PRB of B. braunii race L

Lyophilized *B. braunii* race L material was ultrasonically extracted twice with MeOH, five times with MeOH/CH₂Cl₂ (1/1) and twice with hexane. The residue recovered after these extractions was saponified with 2N KOH in MeOH and extracted. The residue thus obtained was hydrolysed with HCl according to a previously reported procedure [17]. The residue was washed several times with water to remove salts and then dried under vaccum. The highly resistant material isolated, termed PRB L [a], accounted for about 25% of the dry biomass.

Pyrolysis methods

In case of the soluble lipids, samples were directly applied to ferromagnetic wires and the solvent was allowed to evaporate at elevated temperatures using an infrared lamp under a nitrogen atmosphere. The algaenan sample from the race L was pressed onto a flattened ferromagnetic wire. The samples were heated by inductive heating of the ferromagnetic wires (Curie temperatures 610 or 770°C for pyrolysis and 358°C for thermal extraction) for 10 s using a Curie point high-frequency generator (Fischer 9425). The glass tube in which the ferromagnetic wire is positioned was surrounded by a ceramic tube which was independently heated to 250°C. The gas chromatograph (Hewlett Packard HP-5890) was equipped with a cryogenic unit and programmed from 0°C (5 min) to 320°C (10 min) at a rate of 3°C/min. Separation of the products was achieved by a 25 m fused silica capillary column coated with chemically bound CP-Sil 5 (0.32 mm i.d.; film thickness 0.45 μm). Helium was used as carrier gas and the temperature of the flame ionisation detector (FID) was 320°C.

Py–GC/MS was performed using the same pyrolysis and GC conditions. The column was coupled to the EI ion source of a VG-70S double focusing mass spectrometer (mass range m/z 40–800; cycle time 1.8 s; ionization energy 70 eV).

Gas chromatography

GC was performed with a Carlo Erba 4160 instrument equipped with an FID and an on-column injector. A fused silica capillary column

---

[a] The term PRB L was previously attributed to material isolated from the race L following a procedure that was only different for the acid treatment; concentrated phosphoric acid was used instead of hydrochloric acid in the present study.

(25 m × 0.32 mm) coated with CP Sil-5 (film thickness 0.45 μm) was used with helium as carrier gas. The oven was programmed from 70 to 320°C at 4°C/min.

High-temperature GC (HT-GC) was performed with the same instrument. The samples were directly injected into a 10 m fused silica capillary column coated with chemically bound CP-Sil 5 (0.32 mm i.d.; film thickness 0.45 μm). Helium was used as carrier gas and the oven was programmed from 75 to 200°C at 20°C/min, and then at a rate of 6°C/min to 375°C, at which temperature it was held for 10 min.

Gas chromatography/mass spectrometry and probe-mass spectrometry

GC/MS and HT-GC/MS analyses were performed using the same conditions as described for GC and HT-GC, respectively, using a Hewlett Packard gas chromatograph (HP-5890). The column was directly inserted into the ion source of a VG-70S mass spectrometer (mass range m/z 40–800 for GC/MS and m/z 50–1000 for HT-GC/MS; cycle time 1.8 s; ionisation energy 70 eV).

Probe-MS analyses were performed implementing a direct probe inlet and the same mass spectrometer, using a mass range m/z 40–1000 with a cycle time of 1.8 s and an ionization energy of 70 eV. The probe was heated gradually at a rate of 200°C/min.

RESULTS AND DISCUSSION

Alkenyl–phenols

Fig. 2(A) shows the chromatogram of the compounds derived from the alkenyl–phenols **1** using a Curie temperature of 770°C. Identification of these compounds by mass spectrometry after Py–GC/MS analysis indicated the presence of n-alkanes ranging from C_{12} to C_{22}, C_9 to C_{13} alkyl-substituted benzenes (alkylbenzenes occurring as contaminants in linear alkylbenzene sulphonates (LAS) [19]), phthalate and squalene. Based on previous studies [12] it was clear that none of these compounds could have been generated by pyrolysis of **1**. Moreover, expected pyrolysis products of **1**, such as compounds containing a dimethoxyphenol moiety, were not found. Therefore, these results strongly suggest that pyrolysis of **1** had not occurred or that the pyrolysis products were not transferred to the GC column.

The n-alkanes, alkylbenzenes, phthalate and squalene were thus ascribed to minor compounds present as such in the samples which thermally evaporated upon heating. This interpretation was substantiated by the results of subsequent GC analyses using ferromagnetic wires with a Curie temperature of 358°C as injector device (Fig. 2(B)); essentially the same distributions of n-alkanes, alkylbenzenes, phthalate and squalene were observed.
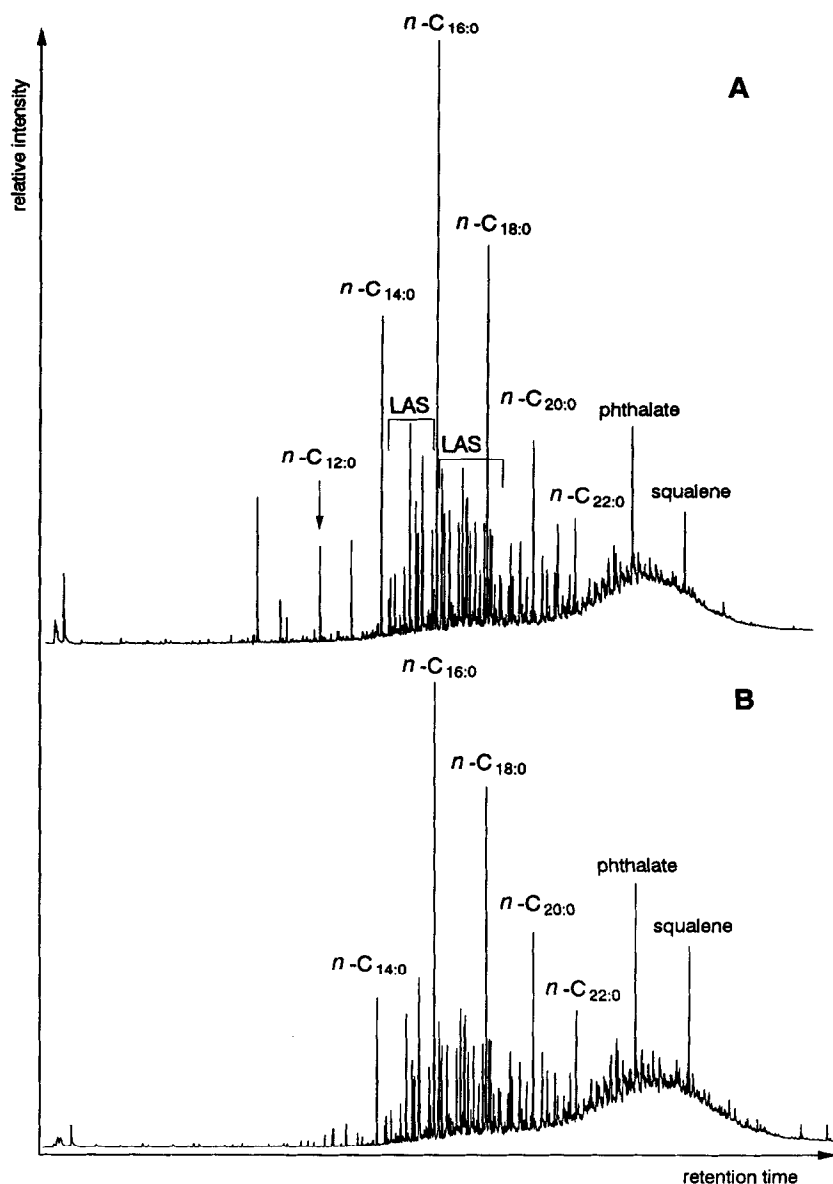
Fig. 2. Gas chromatograms of compounds encountered after subjecting compounds **1** to pyrolysis conditions at (A) 770°C and to evaporation at (B) 358°C. $n\text{-}C_{x:0}$ indicate n-alkanes, x being the carbon number.

To explore the possibility that compounds **1** were not pyrolysed but had evaporated and condensed on the inside of the glass tube, the glass wall surrounding the ferromagnetic wire in the pyrolysis unit was rinsed with dichloromethane to recover any condensed residue. Probe-MS of this material clearly indicated that compounds **1** indeed had evaporated and that no
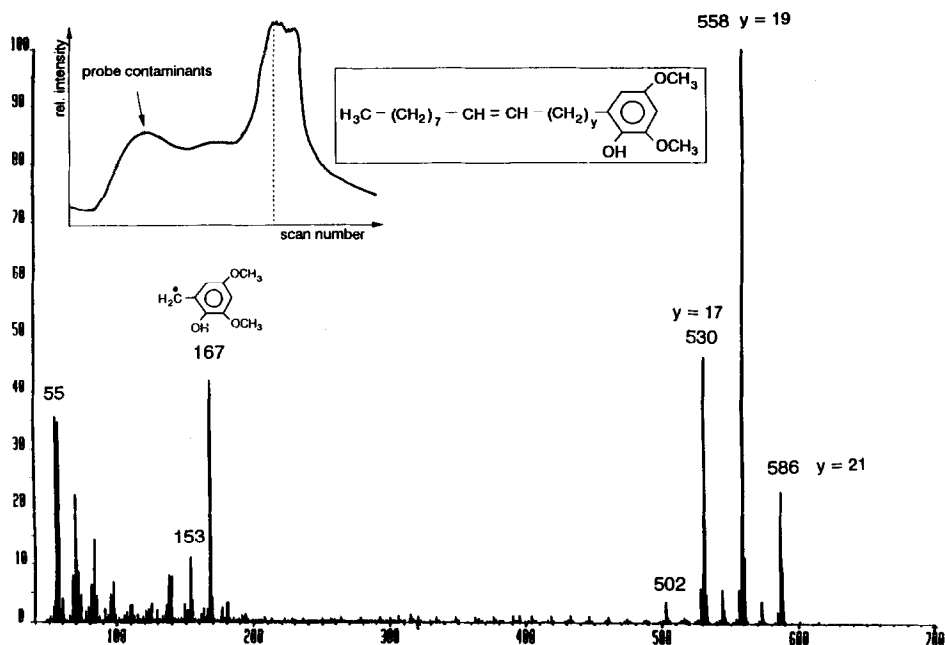
Fig. 3. Probe-mass spectrum of the residue obtained by rinsing the glass tube after subjecting compounds 1 to pyrolysis conditions at 770°C. The curve shown in the upper left part of the Figure indicates the total ion current trace and the dashed line indicates the scan selected for the mass spectrum.

pyrolysis had taken place (Fig. 3); the mass spectra revealed the molecular ions expected and were similar to those previously reported for these compounds [16].

Straightforward GC analyses of the condensed residue further confirmed these probe-MS results (Fig. 4(A)). GC analysis of compounds 1 revealed that n-alkanes, alkylbenzenes, phthalate and squalene only represent a very small amount of the sample (Fig. 4(B)). The absence of highly volatile compounds (C_9–C_{13}) in the compound mixtures obtained in the experiments using the ferromagnetic wires is likely to be due to their pre-evaporation during the gentle heating of the wires, before they are introduced into the pyrolysis unit.

We have to conclude that compounds 1 cannot be analysed either as pyrolysate or as evaporate because of their condensation onto the relatively cold glass wall (250°C) after evaporation from the wire; they were not transferred to the GC column.

Botryals

The C_{52}–C_{64} botryals represent complex lipids with a long straight chain containing a conjugated aldehyde function in the middle (compounds 2 in Fig. 1).
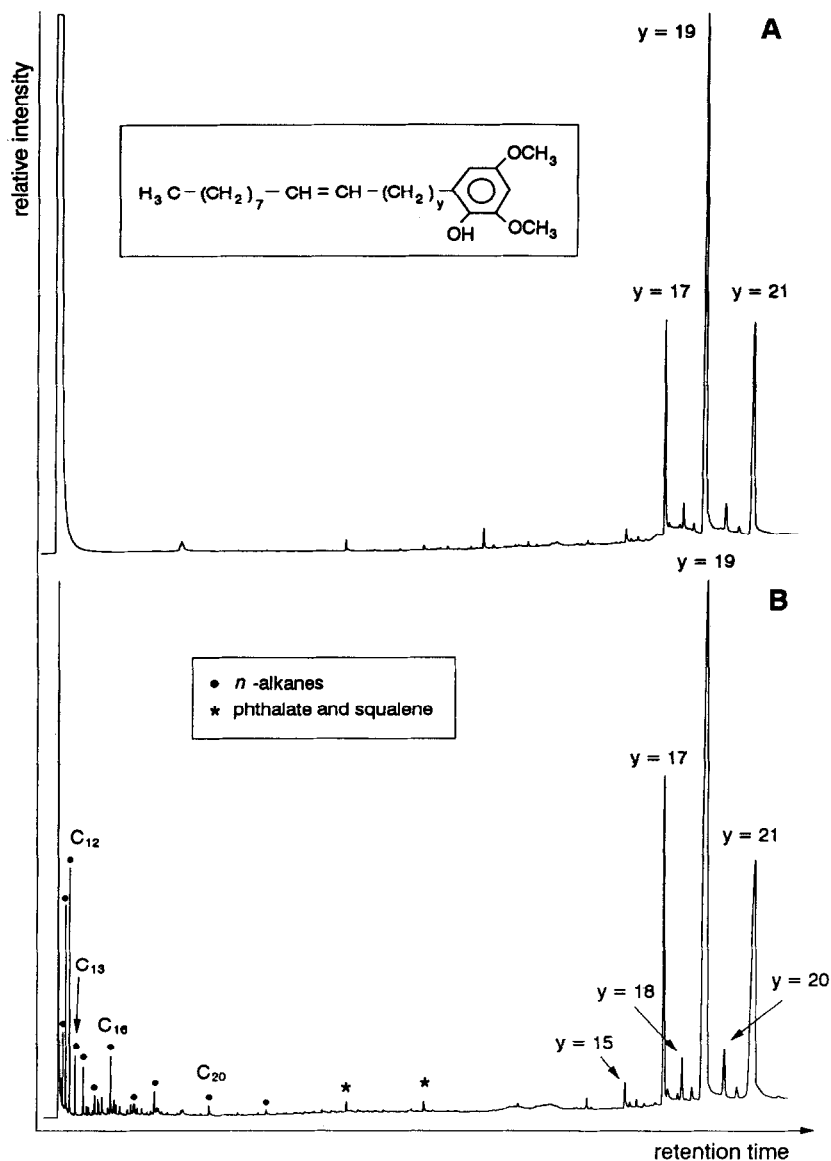
Fig. 4. Gas chromatograms of (A) the condensed residue and (B) compounds 1; (●) n-alkanes, (*) phthalate and squalene.

Figure 5(A) shows the compounds obtained after Py–GC at 610°C. The three major compounds were identified as $C_{16:0}$, $C_{18:1}$ and $C_{18:0}$ primary alcohols. The other components represented by this chromatogram were mainly series of n-alkanes, octadecenamide and phthalates. Since the alcohols and the other compounds observed are difficult to explain by pyrolysis of the botryals, identical behavior to that observed for compounds 1 seemed
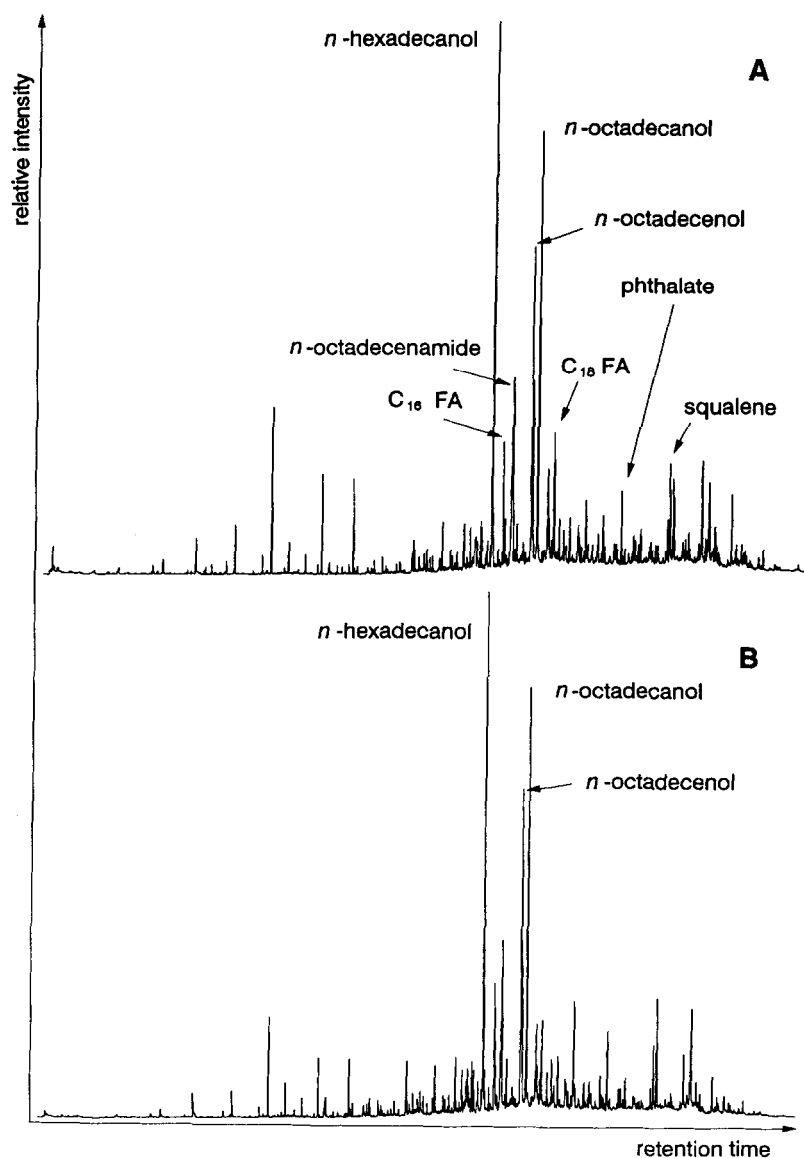
Fig. 5. Gas chromatograms of compounds encountered after subjecting compounds 2 to (A) pyrolysis conditions at 610°C and (B) evaporation at 358°C.

likely. Using a wire with a Curie temperature of 358°C (Fig. 5(B)) indeed showed very similar distributions of the compounds found in the experiment at 610°C, indicating that these compounds represent small amounts of evaporated lipids not related to the botryals. It is assumed that the alcohols and octadecenamide originate from the alga itself and were not separated from the botryals during the isolation process.

The glass tube was rinsed after the 610°C experiment and the condensed residue recovered was analysed by high-temperature gas chromatography (HT-GC). This analysis revealed the almost exclusive presence of compounds **2**. To determine the relative abundance of the impurities in the sample of compounds **2**, HT-GC/MS analysis was performed on both the condensed residue and the unheated sample. In the TIC trace of the latter, most of the impurities dominantly present in the Py–GC analysis were found in trace quantities only (Fig. 6(A)). Figure 6(B) shows a typical mass spectrum of the C_{60} botryals obtained by HT-GC/MS. The molecular ion peak at m/z 850 is very intense, indicating the intact structure of the C_{60} botryals.

Despite their long chain length, the high molecular weight and the presence of functional groups, the botryals, like the alkenyl–phenols **1**, evaporated before pyrolysis could take place, but their transfer to the GC column was hampered by condensation on the relatively cold glass tube.

Alkatrienyl–alkadienyl ether lipids

The pyrolysis behavior of long-chain alkylethers related to the alka-trienyl–alkadienyl ether lipids indicated in Fig. 1 (compounds **3**) has recently been discussed [12]. The cleavage of the C–O ether bond was considered as an important first step in the pyrolysis process.

The TIC trace of the flash pyrolysate of compounds **3** at 770°C (Fig. 7(A)) reveals the presence of C_7, C_9, C_{16}, C_{17} and C_{18} aldehydes, C_{27} linear hydrocarbons and ketones, series of alk-1-enes and α, ω-alkadienes, and a series of even carbon numbered *n*-alkanes.

Most of these compounds are pyrolysis products **3**, because thermal evaporation at 358°C of compounds **3** mainly revealed the series of *n*-alkanes (Fig. 7(B)). As previously observed for compounds **1** and **2**, these alkanes probably represent impurities in the sample which evaporate. The HT-GC-FID trace revealed that the alkanes were indeed present in a low amount. A large difference in the relative abundances of the alkanes was revealed by the Py–GC and the HT-GC traces (compare Figs. 7(A) and 8(A)). This suggests that compounds **3** are only partly pyrolysed, resulting in an overestimation of the alkane impurities reflected by the Py–GC trace. HT-GC analysis clearly indicates that the residue recovered from the glass tube is composed almost exclusively of compounds **3**. This observation proved that a substantial portion of these ether lipids did not pyrolyse, but evaporated and condensed before transfer to the GC column.

The integral structure of ether lipid **3** ($y = 15$) was confirmed by the mass spectrum obtained through HT-GC/MS analysis (Fig. 8(B)). The base peak at m/z 513 results from cleavage of the bond between the oxygen-bearing carbon atoms. The two other major fragmentations are due to loss of H_2O (m/z 762), and loss of H_2O followed by loss of C_6H_{13} (m/z 677).
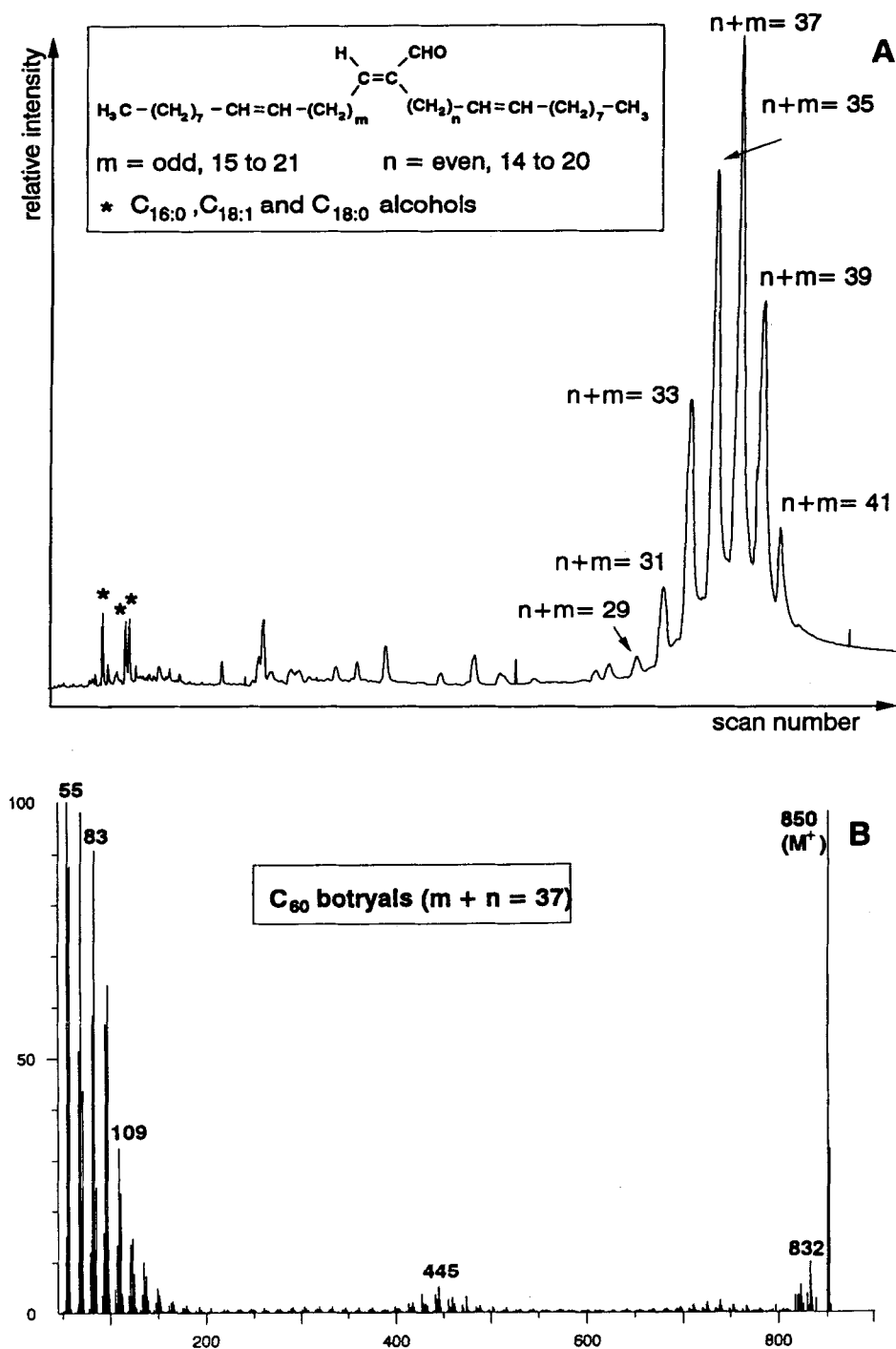
Fig. 6. (A) TIC trace of compounds **2** obtained through HT-GC; (*) $C_{16:0}$, $C_{18:1}$ and $C_{18:0}$ alcohols. (B) Mass spectrum of the C_{60} botryals obtained by HT-GC/MS of the residue condensed in the glass tube after treatment of compounds **1** at 610°C.
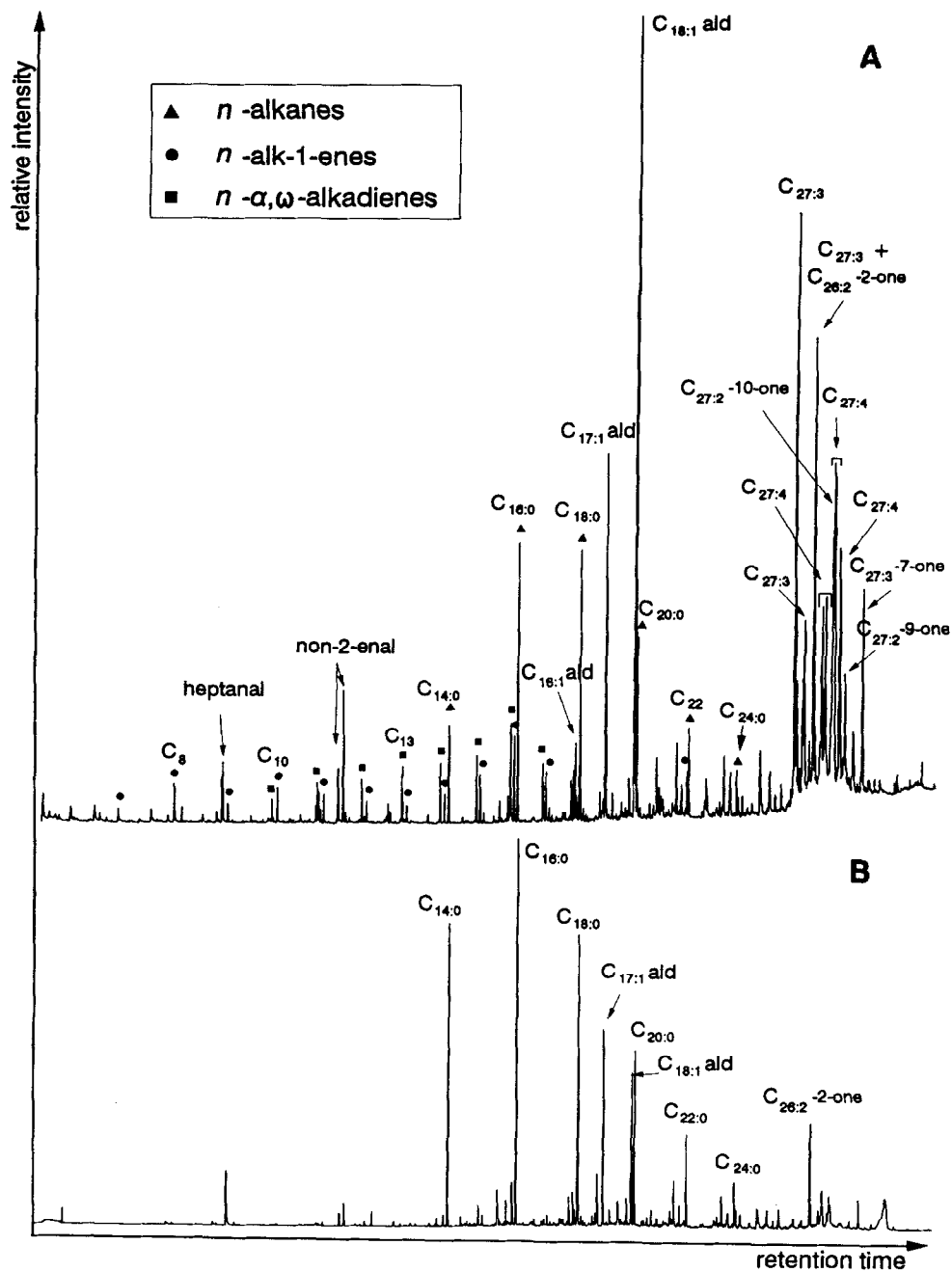
Fig. 7. TIC trace of the compounds encountered after subjecting compounds 3 to (A) pyrolysis at 770°C and (B) evaporation at 358°C.
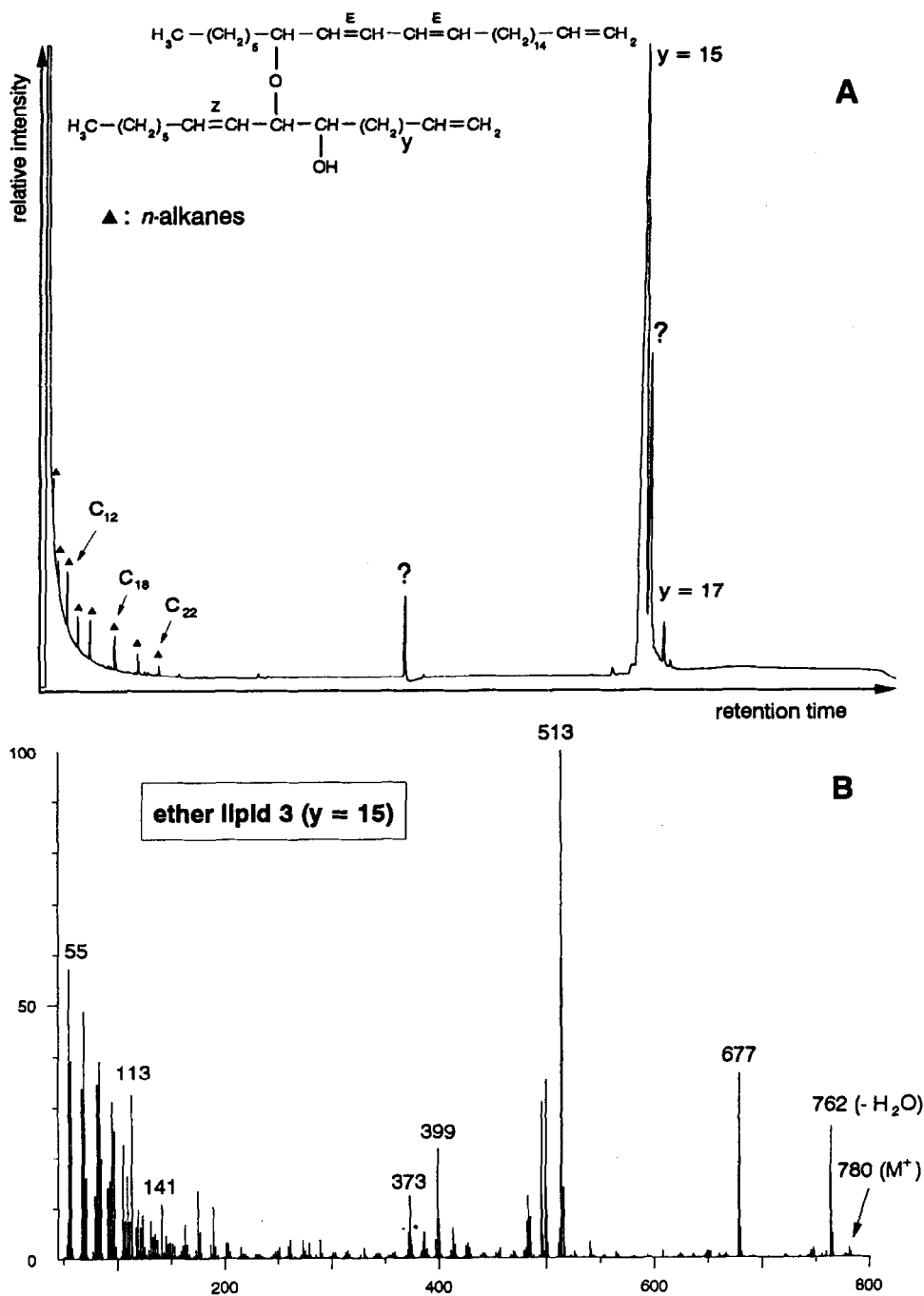
Fig. 8. (A) High-temperature gas chromatogram of compounds **3**; (▲) series of *n*-alkanes. (B) mass spectrum of compound **3** ($y = 15$) obtained by HT-GC/MS.

Apart from the alkanes, most of the other compounds encountered after pyrolysis of compounds **3** are true pyrolysis products. Figure 9 rationalizes the formation of most of these pyrolysis products by assuming four major cleavages. The presence of the major product, octadec-17-enal is probably triggered by cleavage $\langle 1 \rangle$. The radical formed can be stabilized as the aldehyde by an intermolecular H radical transfer. Non-2-enal and heptanal are produced by two successive bond cleavages: $\langle 1 \rangle + \langle 3 \rangle$ and $\langle 2 \rangle + \langle 4 \rangle$ generate non-2-enal and heptanal, respectively. Cleavages $\langle 2 \rangle$ and $\langle 3 \rangle$ lead to the formation of various C_{27} compounds, most of them present in the pyrolysates. The introduction of unsaturations in the structures of these products induces the formation of various isomers of heptacosatriene and heptacosatetraene. Those represented in Fig. 9 are the products generated upon cleavage and H radical transfer, sometimes in combination with loss of H_2O.

The mid-chain ketones indicated in Fig. 9 were identified by their relative retention times and their characteristic mass spectra. Their formation is rationalized by C–O cleavage $\langle 2 \rangle$ followed by hydrogen abstraction and by C–O cleavage $\langle 3 \rangle$, followed by dehydration and H radical addition. It should be noted that the position of the keto groups are in full agreement with the location of the ether linkages in compounds **3**.

Alkenyl–botryal ether lipids

The alkenyl–botryal ethers (compounds **4** in Fig. 1) were not amenable by HT-GC/MS analyses due to their high molecular weight (> 1400 D) and probe-MS analyses failed to produce the molecular ion peaks [14]. Therefore, studies of the condensed residue obtained after Py–GC experiments did not give any information concerning the efficiency of the pyrolysis. Although the probe-mass spectrum of the condensed residue showed high abundances of peaks in the mass area of the botryal molecular ion peaks, it was not possible to establish if these peaks represented molecular ions of "botryal-like" compounds produced by pyrolysis of **4** or if they were fragment ions of the ether lipids **4** which were partly evaporated and condensed. Figure 10 shows the TIC trace of the pyrolysate of compounds **4**. Oleic and palmitic acids, as discussed previously, are thought to be derived from a six-membered ring rearrangement triggered by the ester functionality [12]. Expected cleavages near the ether bond obviously occurred and result in the formation of C_{27}, C_{29} and C_{31} compounds. However, based on the absence of even carbon numbered carbon compounds, it seems that no further pyrolysis of the botryal moieties occurred: almost all the compounds present in the pyrolysates represent the C_{27}, C_{29} and C_{31} alkyl moieties. The three cleavages leading to the formation of most of the pyrolysis products are shown in Fig. 11. Cleavage $\langle 1 \rangle$ followed by H radical transfer explains the formation of the C_{18}, C_{20} and C_{22} ω-alkenals,
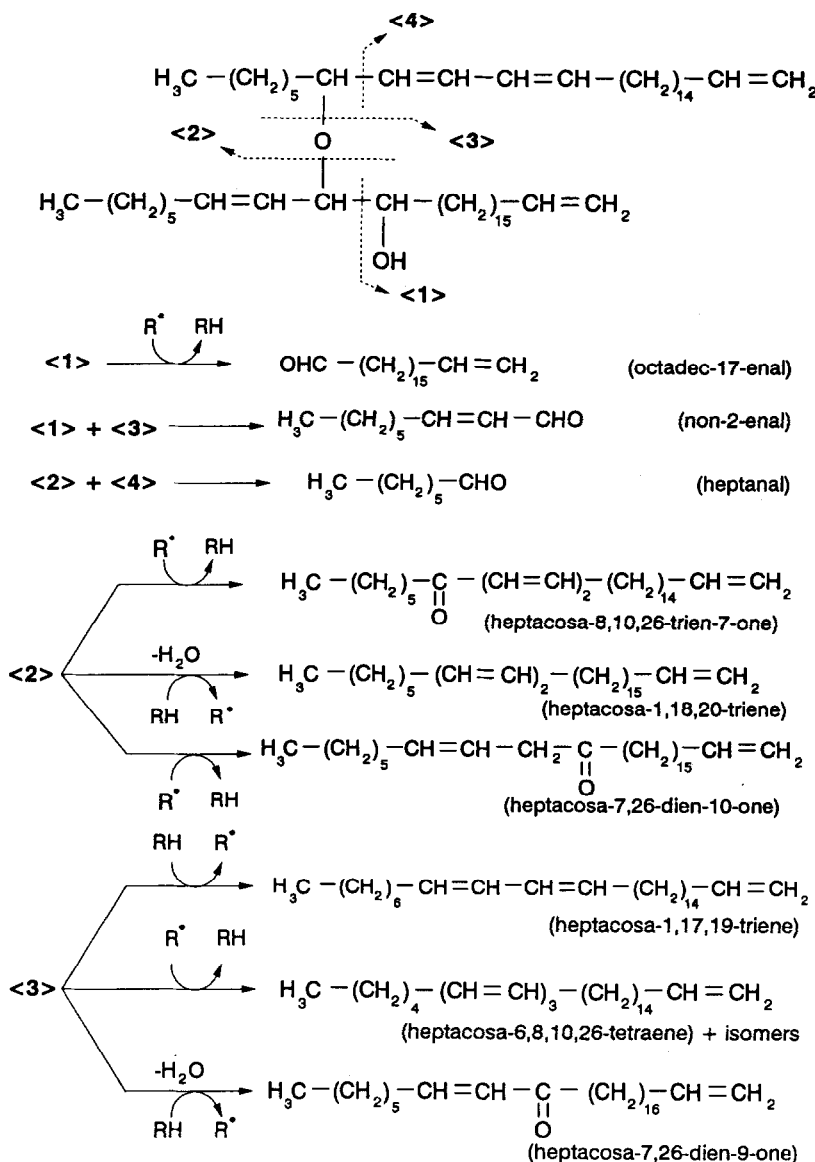
Fig. 9. Proposed mechanisms of pyrolysis for the formation of the major products found in the pyrolysate of compounds 3.

and cleavages $\langle 1 \rangle + \langle 3 \rangle$ may explain the formation of nonanal. The formation of the alkadiones was probably induced by cleavage $\langle 3 \rangle$ followed by H radical transfers. The C_{27}, C_{29} and C_{31} alken-9-ones are generated via cleavage $\langle 3 \rangle$ followed by dehydration and H radical transfer. The major component in the pyrolysate, nonacosadiene, is probably produced by cleavage $\langle 2 \rangle$ and subsequent dehydration. This reaction sequence also explains the formation of C_{27}, C_{29} and C_{31} alken-10-ones and alkatrienes.
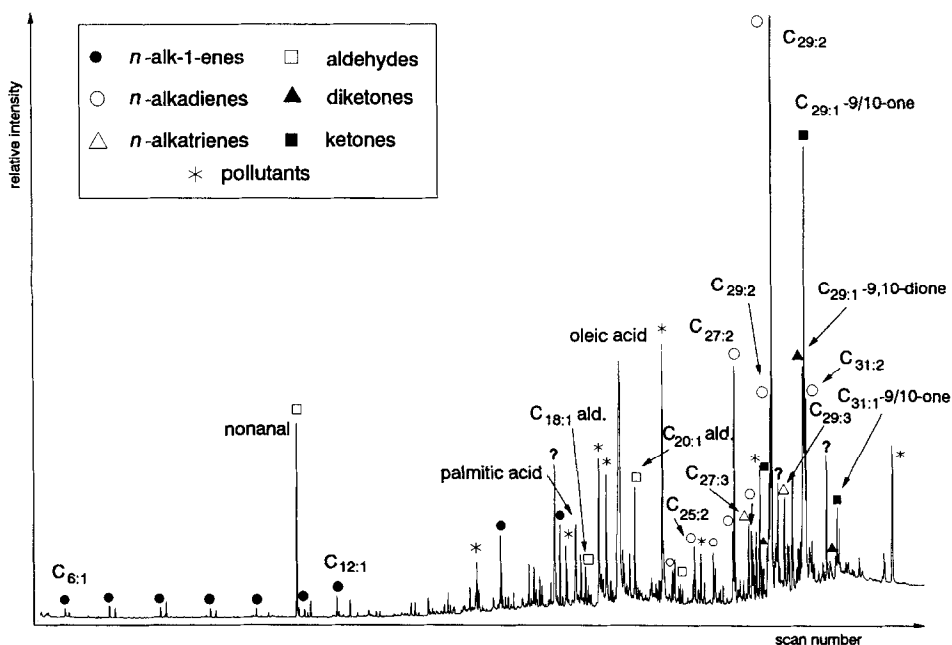
Fig. 10. Total ion current trace of the flash pyrolysate of compounds **4** (Curie temperature 610°C).

More detailed mechanisms of pyrolysis for the formation of these types of compounds and identifications of ketones and diketones are reported by Gelin et al. [12].

PRB L

The resistant biopolymer of *B. braunii* race L was studied previously by spectroscopic methods and off-line pyrolysis experiments [20,21]. It was demonstrated that the structure of this macromolecule is mainly composed of C_{40} isoprenoid units with the isoprenoid lycopane skeleton linked via ether bridges. However, a precise structure could not be proposed based on the results of these experiments.

The TIC trace of the flash pyrolysate of the PRB L showed several series of alkanes and alkenes (Fig. 12). *n*-Alkanes and *n*-alk-1-enes were present in relatively low amounts and ranged from C_7 to C_{21}. The occurrence of these two series seems to indicate that at least a small part of the PRB L consists of long, linear methylene chains similar to those found in the PRB of races A and B of *B. braunii*. The two major series of pyrolysis products are isoprenoid alkenes ranging from C_9 to C_{21} and alkanes ranging from C_{10} to C_{18}. Apart from these series, phyt-2-enes were found in relatively large amounts. The mass spectrum of the major product of the pyrolysate was indicative of 6,10,14-trimethylpentadecan-2-one. Another important car-
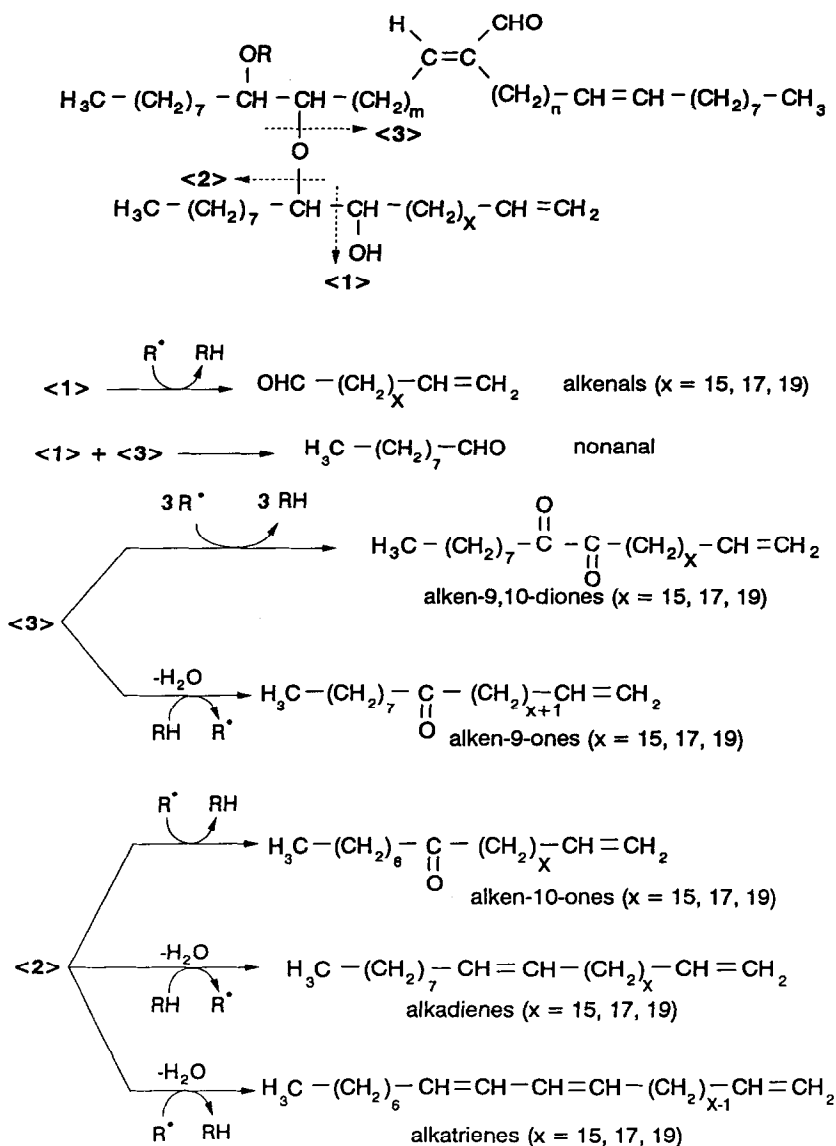
Fig. 11. Proposed mechanisms of pyrolysis for the formation of some of the major products found in the pyrolysate of compounds 4.

bonyl compound was the C_{22} aldehyde whose spectrum showed a major fragment ion at m/z 98 (Fig. 13(A)). Similar fragmentations for γ-unsaturated aldehydes can be explained by a six-membered ring rearrangement involving the carbonyl. Fragmentations at $M^+ - 18$, $M^+ - 43$ and $M^+ - 44$ confirmed the presence of the aldehyde moiety. Among the HMW pyrolysis products (Fig. 12, insert), alkadienes and unsaturated ketones with 40
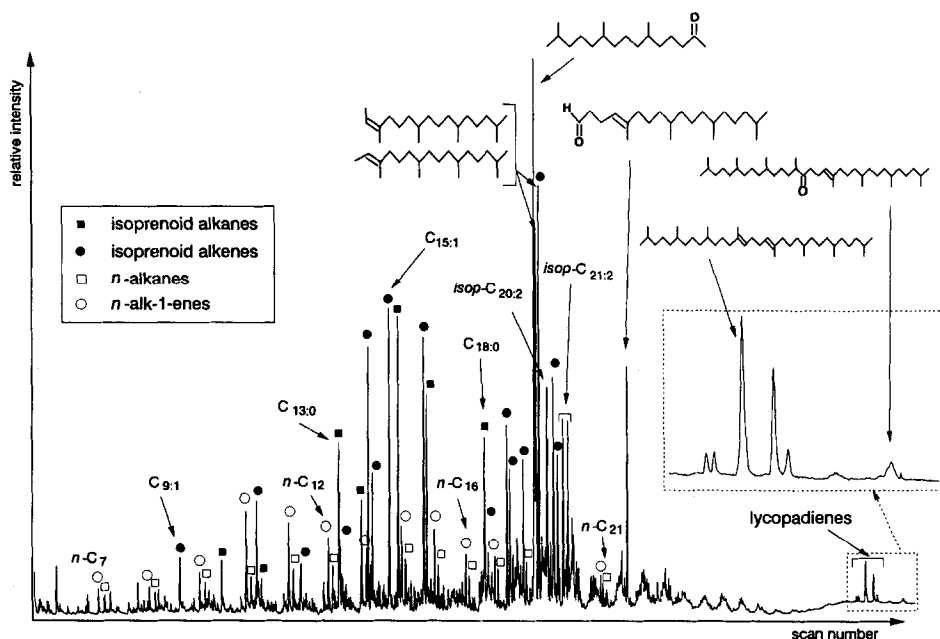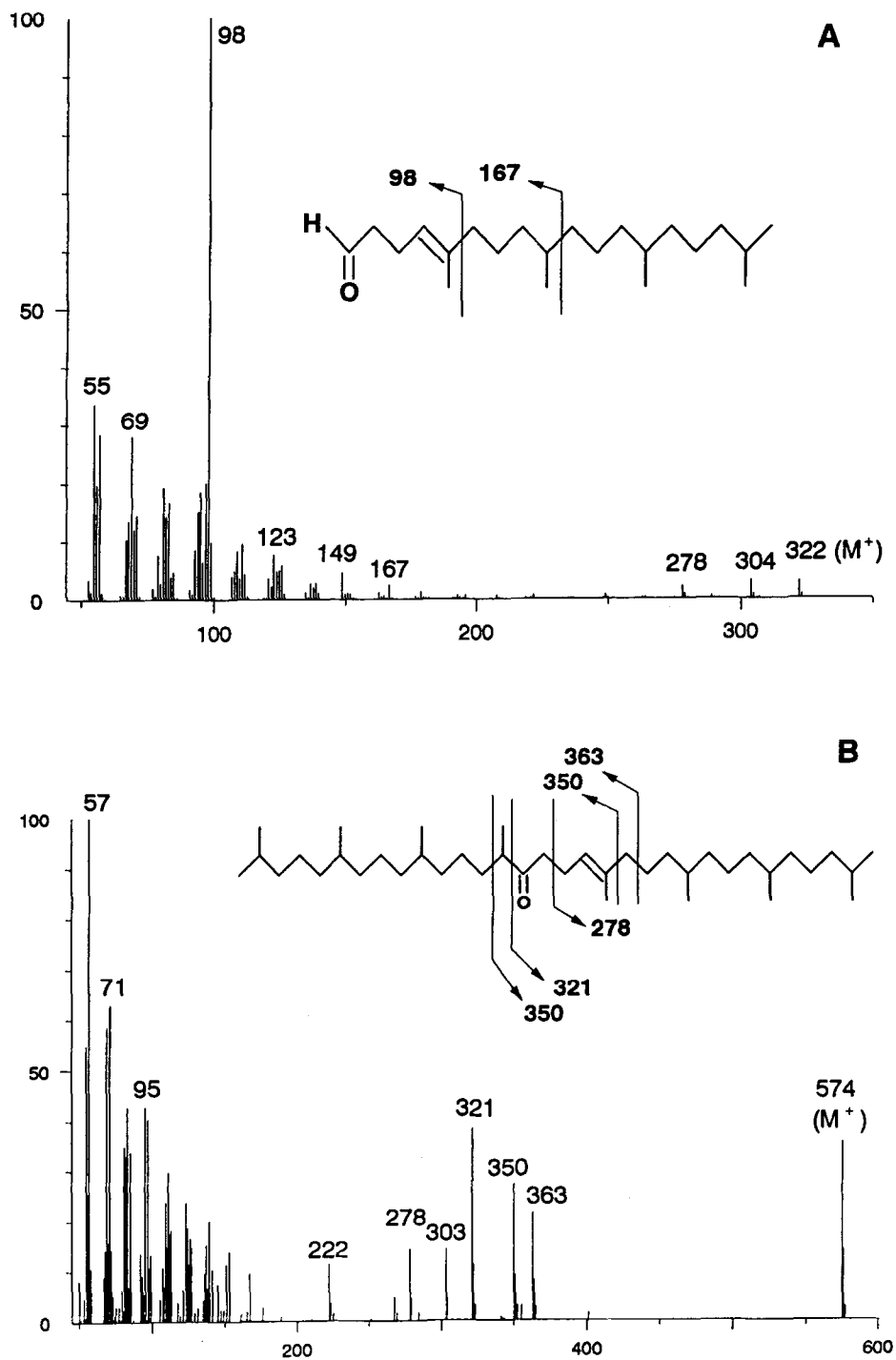
Fig. 12. TIC trace of the flash pyrolysate of PRB L (Curie temperature 610°C).

carbons were identified. The structure of one of the C_{40} alkadienes indicated in Fig. 12 was determined in a previous study [22]. The positions of the double bonds in the other lycopadienes could not be determined by mass spectrometry. It should be noted that *B. braunii* race L produces only one hydrocarbon, a C_{40} isoprenoid lycopadiene, which was identified as 2,6(R),10(R),14,19,23(R),27(R),31-octamethyldotriaconta-14(E),18(E)-diene [22]. The C_{40} ketone identified was present in small amounts; Fig. 13(B) shows its mass spectrum. The structure indicated was determined by specific mass spectrometric fragment ions, most likely derived from 2,6,10,14,19, 23,27,31-octamethyldotriacont-14-en-18-one (Fig. 13(B)).

The presence of the three oxygen-containing compounds and lycopadienes described above strongly indicates that similar cleavages to those observed during pyrolysis of the ether lipids studied in this paper also occurred in PRB L. The positions of the ether bonds at C(14) and C(15) as indicated in Fig. 14 are supported by the generation of both the C_{18} alkan-2-one and C_{40} alken-15-one, and the production of the C_{22} aldehyde. A partial structure of the polymer comprising the major part of the PRB L is proposed in Fig. 15. The five cleavages indicated rationalize the formation of the four compounds already discussed. The clue to the reconstruction of the polymer structure proposed was the formation of the C_{22} aldehyde via a pathway similar to that described for the formation of nonanal during the pyrolysis of compounds **4**. The hypothetical formation of the C_{40} alcohol

Fig. 13. Mass spectra of (A) 5,9,13,17-tetramethyloctadec-4-enal and (B) 2,6,10,14,29,23, 27,31-octamethyldotriacont-14-en-18-one.
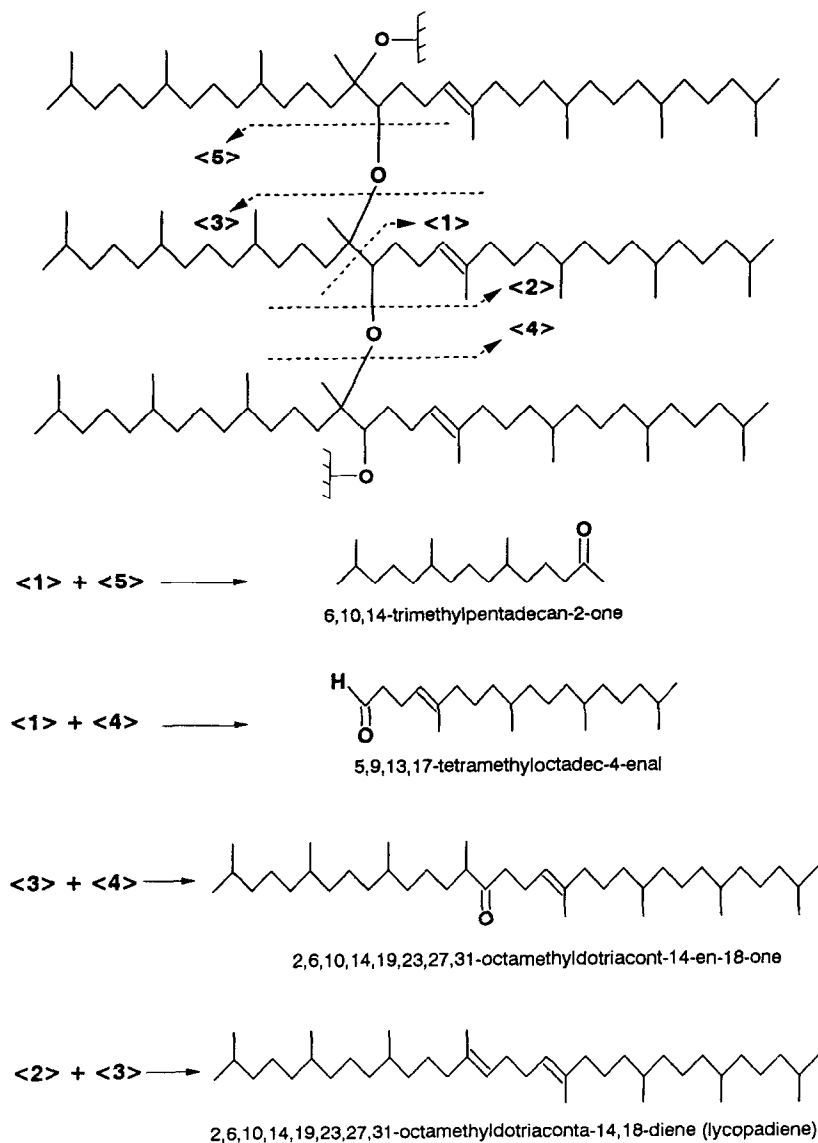
Fig. 14. Proposed structure for the major biopolymer of PRB L; (---→) some major cleavages occurring upon pyrolysis leading to the formation of 6,10,14-trimethylpentadecan-2-one, 5,9,13,17-tetramethyloctadec-4-enal, 2,6,10,14,19,23,27,31-octamethyldotriaconta-14,18-diene and 2,6,10,14,19,23,27,31-octamethyldotriacont-14-en-18-one.

with the hydroxyl group at the C(14) position would probably be followed by a dehydration, thus generating the lycopadienes.

It should be noted that the structure of PRB L proposed here, and essentially based on mechanisms of Curie point pyrolysis of ether lipids, is

in full agreement with data obtained in other pyrolysis studies aiming to study changes of these type of polymers during burial in the earth under various temperature and time conditions [23].

CONCLUSIONS

1 To interpret Py–GC and Py–GC/MS data of HMW lipids, it is a prerequisite to analyse constituents left behind in the pyrolysis unit to check on evaporation versus pyrolysis and to be alert to transfer problems from the pyrolysis chamber to the GC column.

2 HT-GC and HT-GC/MS are powerful methods of analysing HMW lipids which appear to be thermostable.

3 Detailed investigations of pyrolysis mechanisms of well-selected model compounds are needed to optimally benefit from pyrolytic analysis methods.

4 A detailed structure was proposed for a natural algal biopolymer partly based on flash Py–GC/MS analysis. To the best of our knowledge, it is the first time that a precise structure could be determined by this analytical method.

REFERENCES

1 D. van de Meent, S.C. Brown, R.P. Philip and B.R.T. Simoneit, Geochim. Cosmochim. Acta, 44 (1980) 999.
2 S.R. Larter, in K.J. Voorhees (Ed.), Analytical Pyrolysis, Butterworths, London, 1984, p. 212.
3 E.W. Tegelaar, J.W. de Leeuw, S. Derenne and C. Largeau, Geochim. Cosmochim. Acta, 53 (1989) 3103.
4 E.W. Tegelaar, R.M. Matthezing, J.B.H. Jansen, B. Horsfield and J.W. de Leeuw, Nature, 342 (1989) 529.
5 K. Goth, J.W. de Leeuw, W. Püttmann and E.W. Tegelaar, Nature, 336 (1988) 759.
6 S. Derenne, C. Largeau, E. Casadevall, C. Berkaloff and B. Rousseau, Geochim. Cosmochim. Acta, 55 (1991) 1041.
7 C. Largeau, S. Derenne, E. Casadevall, A. Kadouri and N. Sellier, in D. Leythaeuser and J. Rullkotter (Eds.), Advances in Organic Geochemistry 1985, Org. Geochem., Vol. 10, Pergamon, Oxford, 1986, pp. 1023–1032.
8 S. Derenne, C. Largeau, E. Casadevall and J. Connan, Org. Geochem., 12 (1988) 43.
9 C. Dubreuil, S. Derenne, C. Largeau, C. Berkaloff and B. Rousseau, Org. Geochem, 14 (1989) 543.
10 J.-P. Gatellier, J.W. de Leeuw, J.S. Sinninghe Damsté, S. Derenne, C. Largeau and P. Metzger, Geochim. Cosmochim. Acta, 57 (1993) 2053.
11 J.S. Sinninghe Damsté, F.X.C. de las Heras, P.F. van Bergen and J.W. de Leeuw, Geochim. Cosmochim. Acta, 57 (1993) 389.
12 F. Gelin, J.-P. Gatellier, J.S. Sinninghe Damsté, P. Metzger, S. Derenne, C. Largeau and J.W. de Leeuw, J. Anal. Appl. Pyrolysis, 27 (1993) 155.
13 F. Gelin, J.W. de Leeuw, J.S. Sinninghe Damsté, S. Derenne, C. Largeau and P. Metzger, Org. Geochem., in press.

14 P. Metzger, C. Largeau and E. Casadevall, Prog. Chem. Org. Nat. Prod., 57 (1991) 1–70.
15 P. Metzger and E. Casadevall, Phytochemistry, 28 (1989) 2097.
16 P. Metzger and E. Casadevall, Phytochemistry, 30 (1991) 1439.
17 P. Metzger and E. Casadevall, Phytochemistry, 31 (1992) 2341.
18 H. Goossens, J.W. de Leeuw, W.I.C. Rijpstra, G.J. Meyburg and P.A. Schenck, Org. Geochem., 14 (1989) 15–25.
19 G.R. Harvey, J.S. Sinninghe Damsté and J.W. de Leeuw, Marine Chem., 16 (1985) 187–188.
20 S. Derenne, C. Largeau, E. Casadevall and C. Berkaloff, Phytochemistry, 28 (1989) 1137.
21 S. Derenne, C. Largeau, E. Casadevall and N. Sellier, Phytochemistry, 29 (1990) 2187.
22 P. Metzger and E. Casadevall, Tetrahedron Lett., 28 (1987) 3931.
23 F. Behar, S. Derenne and C. Largeau, Geochim. Cosmochim. Acta, in press.